Mechanisms of Nucleophilic Addition to Activated Double Bonds: 1,2- and 1,4-Michael Addition of Ammonia

Leonardo Pardo,[†,‡] Roman Osman,[‡] Harel Weinstein,[*,‡] and James R. Rabinowitz[§]

Contribution from the Department of Physiology and Biophysics, Mount Sinai School of Medicine of the City University of New York, New York, New York 10029, and Environmental Protection Agency, Research Triangle Park, North Carolina 27711

Received November 30, 1992

Abstract: The molecular mechanisms for nucleophilic addition of an ammonia molecule to three small molecules with activated double bonds—acrolein (ACR), acrylonitrile (ACN), and acrylic acid (AA)—have been examined with ab initio quantum chemical methods in reactions modeling their interactions with biological targets. The calculations include the nucleophilic addition reaction of either an ammonia molecule or an NH_3 hydrogen bonded to a discrete water molecule (NH_3·OH_2) to ACR, ACN, and AA. Optimizations of the geometries of reactants and transition structures for the 1,2- and 1,4-addition mechanisms were done at the restricted Hartree–Fock level with 6-31G basis sets, and electron correlation energy was calculated at the MP2 level with 6-31G* basis sets. Reaction energies were corrected for zero-point energies calculated from the harmonic vibrational frequencies of the 6-31G optimized structures. Hydration enthalpies were evaluated with the solvent described as a polarizable dielectric continuum. The barriers calculated for the addition reactions were found to be significantly reduced by the assistance of a solvent molecule in the intramolecular proton-transfer process. The order of reactivities, based on energies of activation of the 1,4-addition to ACR, either 1,2- or 1,4-addition to AA, and 1,2-addition to ACN, is as follows: ACR > AA > ACN, in very good agreement with experimental results. The results provide inferences regarding the relative capabilities of the molecules in this class to interact with DNA and reflect on their relative potencies in reactions determining the biological effects of these environmentally important chemical species.

Introduction

The nucleophilic addition of amines (e.g., bases of nucleic acids) to the activated double bond of xenobiotics has been suggested as a possible primary event in the mechanism responsible for their biological toxicity (for a recent discussion, see ref 1). Direct addition to DNA in vitro has been demonstrated for such compounds, including acrylonitrile and acrylamide,[2,3] and carcinogenicity as well as mutagenicity were demonstrated for members of this family of enals.[4–6] Because this chemical class includes molecules that have large-volume industrial and consumer applications (e.g., acrylate and methacrylate esters, aldehydes, and ketones), the potential for biological effects due to environmental and human exposure is of significant interest and prompts attempts to understand their mechanisms of interaction with biomolecules.[1] In model studies of such mechanisms, the addition of a fluoride anion to the activated double bond of acrylic acid and methacrylic acid was studied with quantum mechanical calculations in order to determine the source of the difference in reactivity of both molecules.[7] The effect of the charge distribution in such molecules on the reactivity of the negatively charged nucleophile toward the activated double bond was also analyzed from the Laplacian of the charge density.[8] The results from these studies suggested that the acrylate molecule is likely to be more active than the corresponding methacrylate molecule in reactions determined by the nucleophilic addition mechanism. The biological effects of these molecules have been suggested to depend on such mechanisms (see ref 7), and experimental results on acrylate–methacrylate pairs using the mouse lymphoma cell assay are in agreement with these inferences from the computational studies.[9,10]

In order to understand the relationship between the structure and reactivity of molecules incorporating activated double bonds of this kind, we have investigated the nucleophilic Michael addition of an ammonia molecule to acrolein (ACR), acrylonitrile (ACN), and acrylic acid (AA). These compounds were chosen because they are simple species with a wide range of reactivity,[11] with ACR being the most active and ACN the least reactive. Ammonia was chosen as a nucleophilic target for this exploration because it is the smallest molecule that incorporates some of the relevant features of a nitrogen-centered, nucleophilic site on DNA. In addition, experimental data on the addition of amines to activated double bonds[12] can thus be used for comparison with the results from the computational study.

The addition of a neutral amine to an activated carbon–carbon double bond can be described by Scheme I. A nucleophilic attack on the activated double bond in **1** leads to the charge-separated intermediate **2**, which can yield the neutral product **3** through several pathways. In many cases, the significant pathways that lead from **2** to **3** are either deprotonation of the amine moiety to form a negatively charged molecule or intramolecular proton transfer.[12] The possible pathway through initial protonation of the negatively charged carbon to produce a positively charged

* Correspondence to this author.
† Permanent address: Laboratory of Computational Medicine, Department of Biostatistics, Faculty of Medicine, Universidad Autónoma de Barcelona, 08193 Bellaterra, Barcelona, Spain.
‡ New York.
§ North Carolina.

(1) Wang, M.; Nishkawa, A.; Chung, F.-L. *Chem. Res. Toxicol.* **1992**, *5*, 528–531.
(2) Solomon, J. J.; Segal, A. *Environ. Health Perspect.* **1985**, *62*, 227–230.
(3) Solomon, J. J.; Fedyk, J.; Mukai, F.; Segal, A. *Cancer Res.* **1985**, *45*, 3465–3470.
(4) Chung, F.-L.; Tanaka, T.; Hecht, S. S. *Cancer Res.* **1986**, *46*, 1285–1289.
(5) Lutz, D.; Eder, T.; Heudecker, T.; Hemschler, D. *Mutat. Res.* **1982**, *93*, 305–315.
(6) Marnett, L. J.; Hurd, H. K.; Hollstein, M. C.; Levin, D. E.; Esterbauer, H.; Ames, B. N. *Mutat. Res.* **1985**, *148*, 25–34.
(7) Osman, R.; Namboodiri, K.; Weinstein, H.; Rabinowitz, J. R. *J. Am. Chem. Soc.* **1988**, *110*, 1701–1707.
(8) Carrol, M. T.; Cheeseman, J. R.; Osman, R.; Weinstein, H. *J. Phys. Chem.* **1989**, *93*, 5120–5123.
(9) Moore, M. M.; Amtower, A.; Doerr, C.; Brock, K. H.; Dearfield, K. L. *Environ. Mol. Mutagen.* **1988**, *11*, 49–63.
(10) Dearfield, K. L.; Millis, C. S.; Harrington-Brock, K.; Doerr, C. L.; Moore, M. M. *Mutagenesis* **1989**, *4*, 381–393.
(11) Morton, M.; Landfield, H. *J. Am. Chem. Soc.* **1952**, *74*, 3523–3528.
(12) Bernasconi, C. F. *Tetrahedron* **1989**, *45*, 4017–4090.

0002-7863/93/1515-8263$04.00/0

Scheme I[a]

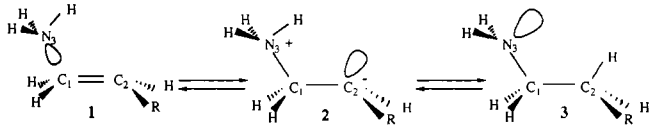

[a] R = CHO, COOH, and CN.

Scheme II[a]

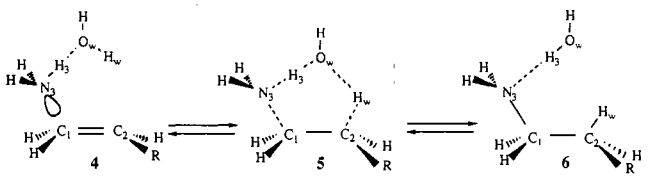

[a] R = CHO, COOH, and CN.

intermediate followed by deprotonation of the amine is not significant.[13] Evidence for the participation of the zwitterionic intermediate **2** in the addition reaction derives from the dependence of the rate and equilibrium constants on both the pK_a of the nucleophilic amine and the capability of the activating group R (see Scheme I) to delocalize the negative charge formed on C_α.[12,14-17] From structure–reactivity relationships, it was shown[18] that the intramolecular proton transfer is a dominant pathway in the addition of amines to activated double bonds, thus establishing the importance of the conversion of the zwitterion **2** to the product **3**. However, the precise mechanism of the intramolecular proton transfer is not known. Several possibilities have been considered, and a direct transfer from the amine to the carbanion has been discounted on the basis of a proton inventory study.[19] On the other hand, a solvent (or reactant-assisted) proton transfer, such as described by **5** in Scheme II, is a feasible mechanism for the intramolecular proton transfer. This suggestion is supported by early observations that in aprotic solvents, addition reactions of this type are second order in the concentration of the amine.[20-22] A recent analysis of the addition of amines to an activated double bond in *trans*-2-furylnitroethylene confirmed the proposed participation of the second amine molecule in the proton transfer in the transition structure.[23] The catalytic role of discrete water molecules in the addition of ammonia to formaldehyde was characterized in a detailed computational study in which the cyclic, activated transition complexes were shown to include one or two solvent molecules.[24]

The computational study presented here is a detailed examination of the molecular mechanisms for nucleophilic addition of an ammonia molecule to three small molecules with activated double bonds. In each case, the electron-withdrawing group affects differently the reactivity of the molecule in the addition reaction. Several mechanisms were explored, leading to the general conclusion that the barriers for the addition reaction are significantly reduced by the assistance of a solvent molecule in the intramolecular proton-transfer process. The results provide inferences regarding the relative capabilities of the molecules in this class to interact with DNA as a function of their specific electron-withdrawing groups.

Methods

All the ab initio quantum mechanical calculations were performed with the GAUSSIAN system of programs, versions 86 and 90.[25] Semiempirical quantum mechanical calculations were performed with the MOPAC program using the AM1 Hamiltonian.[26]

The simulation of the nucleophilic addition of either ammonia or ammonia hydrogen bonded to a discrete water molecule (NH_3·OH_2) to ACR, AA, and ACN includes structure optimizations of reactants and transition structures (TS) at the level of restricted Hartree–Fock calculations with the 6-31G basis set. Characterization of critical points in the potential energy surface was carried out through diagonalization of the Hessian matrix. Electron-correlation energy was calculated with the 6-31G* basis set at the MP2 level with the core orbitals frozen. All one-electron properties, such as Mulliken populations, were calculated from the HF/6-31G* wave function.

The parameters chosen to characterize the nucleophilic addition are E_{act}, which is the barrier for the nucleophilic addition and is defined as the difference in energy between the TS and the reactants, E_{inter}, which is the difference in energy between any intermediate created in the reaction path and the reactants, and E_{react}, which is the difference in energy between the products and the reactants. The system NH_3·OH_2 was constructed to leave the lone pair of the nitrogen free for the nucleophilic attack. Thus, the ammonia is the hydrogen donor, and the oxygen of water is the hydrogen acceptor (NH··O hydrogen bond instead of N··HO). E_{act}, E_{inter}, and E_{react} were corrected for zero-point energies (ZPE) calculated from the harmonic vibrational frequencies of the 6-31G optimized structures.

Hydration enthalpies (E_{solv}) were calculated with the method developed by Rashin[27] in which the charge distribution of the solute is represented by a collection of point charges and the solvent is described as a polarizable dielectric continuum. In this formulation, the enthalpy of solvation is the sum of two terms: the energy required for cavity formation and the electrostatic interaction energy between the charge distribution of the solute molecule and the reaction field it induces in the surrounding dielectric medium.

Results and Discussion

Structure of Reactants. The ab initio calculations of the equilibrium structures of ACR, ACN, and AA were carried out with full geometry optimization with the 6-31G basis set. The equilibrium geometries are virtually identical to those obtained in other theoretical studies.[28] The structures are also in agreement with experimental values.[29] The minimum energy structure of ACR corresponds to the *s-trans* conformation, which has been found to be more stable in both theoretical[28] and experimental[30] studies. From the four possible planar conformers of AA, the *s-cis,syn* was used as the reactant because it was found to be the most stable structure.[28]

Mechanism of the Nucleophilic 1,2-Addition. Experimental evidence indicates that the addition of amines to activated double bonds is second order in the nucleophile.[23] Furthermore, a comprehensive scheme of this process[12] requires the participation

(13) Bernasconi, C. F.; Murray, C. J. *J. Am. Chem. Soc.* **1986**, *108*, 5251–5257.
(14) Bernasconi, C. F.; Fox, J. P.; Fornarini, S. J. *J. Am. Chem. Soc.* **1980**, *102*, 2810–2821.
(15) Shenhav, H.; Rappaport, Z.; Patai, S. *J. Chem. Soc. B* **1970**, *1970*, 469–476.
(16) Bernasconi, C. F.; Leonarduzzi, G. D. *J. Am. Chem. Soc.* **1982**, *104*, 5133–5142.
(17) Bernasconi, C. F.; Carre, D. J.; Kanavariotti, A. *J. Am. Chem. Soc.* **1981**, *103*, 4850–4860.
(18) Bernasconi, C. F.; Murray, C. J. *J. Am. Chem. Soc.* **1986**, *108*, 5257–5264.
(19) Bernasconi, C. F.; Fairchild, D. E.; Murray, C. J. *J. Am. Chem. Soc.* **1987**, *109*, 3409–3415.
(20) Davies, M.; Evans, F. P. *Trans. Faraday Soc.* **1955**, *51*, 1506.
(21) McDowell, S. T.; Stirling, C. J. M. *J. Chem. Soc. B* **1967**, *1967*, 343–347.
(22) Nozaki, K. *J. Am. Chem. Soc.* **1941**, *63*, 2681–2686.
(23) Popov, A. F.; Perepichka, I. F.; Kostenko, L. I. *J. Chem. Soc., Perkin Trans. II* **1989**, *1989*, 395–400.
(24) Williams, I. *J. Am. Chem. Soc.* **1987**, *109*, 6299–6307.
(25) (a) Frisch, M. J.; Binkley, J. S.; Schlegel, H. B.; Raghavachari, K.; Melius, C. F.; Martin, R. L.; Stewart, J. J. P.; Bobrowicz, F. W.; Rohlfing, C. M.; Kahn, L. R.; Defrees, D. J.; Seeger, R.; Whiteside, R. A.; Fox, D. J.; E. M., F.; Pople, J. A. GAUSSIAN 86; Gaussian, Inc.: Pittsburgh, PA, 1986. (b) Frisch, M. J.; Head-Gordon, M.; Trucks, G. W.; Foresman, J. B.; Schlegel, H. B.; Raghavachari, K.; Robb, M. A.; Binkley, J. S.; Gonzalez, C.; Defrees, D. J.; Fox, D. J.; Whiteside, R. A.; Seeger, R.; Melius, C. F.; Baker, J.; Martin, R. L.; Kahn, L. R.; Stewart, J. J. P.; Topiol, S.; Pople, J. A. GAUSSIAN 90; Gaussian, Inc.: Pittsburgh, PA, 1990.
(26) Dewar, M. J. S.; Zabish, E. G.; Healy, E. F.; Stewart, J. J. P. *J. Am. Chem. Soc.* **1985**, *107*, 3902–3909.
(27) Rashin, A. *J. Phys. Chem.* **1990**, *94*, 1725–1733.
(28) Loncharich, R. J.; Schwartz, T. R.; Houck, K. N. *J. Am. Chem. Soc.* **1987**, *109*, 14–23.
(29) Blom, C. E.; Grassi, G.; Bauder, A. J. *J. Am. Chem. Soc.* **1984**, *106*, 7427–7436.
(30) Blom, C. E.; Muller, R. P.; Gunthard, H. H. *Chem. Phys. Lett.* **1980**, *73*, 483–489.

Table I. Selected Geometrical Parameters of Transition Structures (**5**, 1,2-addition; **7**, 1,4-addition), Intermediates (**8**), and Products (**6**) of the Nucleophilic Michael Addition of Ammonia (Scheme IIIa) or $NH_3{\cdot}OH_2$ (Scheme II and IIIb) to ACR, AA, and ACN[a]

	5			**7a**	**7b**		**8a**	**8b**		**6**		
parameters	ACR	AA	ACN	ACR	ACR	AA	ACR	ACR	AA	ACR	AA	ACN
C_1–C_2	1.513	1.516	1.518	1.418	1.490	1.487	1.507	1.503	1.498	1.533	1.531	1.536
C_1–N_3	1.550	1.525	1.538	1.843	1.534	1.530	1.471	1.484	1.488	1.466	1.466	1.464
N_3–H_3	1.081	1.071	1.066	1.015	1.115	1.162	2.000	1.822	1.787	1.962	1.967	1.978
H_3–O_w	1.449	1.495	1.515		1.384	1.308		0.973	0.977	0.962	0.962	0.961
O_w–H_w	1.189	1.211	1.141		1.170	1.223		1.726	1.649	4.019	3.644	3.569
C_2–H_w	1.428	1.402	1.489	2.000[b]	1.211[c]	1.156[c]	0.961[b]	0.969[c]	0.977[c]	1.083	1.082	1.085
N_3–O_w	2.446	2.467	2.485		2.467	2.440		2.739	2.712	2.750	2.903	2.678
O_w–C_2	2.549	2.540	2.555		2.370[d]	2.367[d]		2.675[d]	2.608[d]	3.336	3.259	3.195
N_3–C_1–C_2	111.2	108.9	108.4	107.4	112.4	112.6	112.0	112.4	112.7	110.1	109.7	109.9
H_3–N_3–C_1	106.1	105.3	105.4	95.1	105.0	104.2	95.5	96.9	97.9	97.3	102.2	102.2
O_w–H_3–N_3	149.8	147.6	148.1		161.5	162.2		155.7	156.7	161.0	163.7	160.5
H_w–O_w–H_3	87.3	87.1	87.4		104.2	105.9		105.1	106.6	51.6	56.4	58.8
O_w–H_w–C_2	153.6	152.6	152.3		169.1[e]	168.5[e]		165.3[e]	166.4[e]	44.6	61.0	61.4
H_w–C_2–C_1	100.6	98.2	98.1	99.0[f]	120.2[g]	119.0[g]	111.6[f]	117.5[g]	117.7[g]	110.9	111.0	110.0
C_1–C_2–C_R[j]	116.5	116.2	113.0	116.8	123.1	122.6	125.3	126.4	125.2	111.8	113.3	111.5
H_3–N_3–C_1–C_2	36.3	47.9	47.8	55.4	77.5	76.6	34.9	84.5	82.1	65.1	52.7	50.8
O_w–H_3–N_3–C_1	−33.6	−27.2	−26.7		−5.5	−7.3		−4.4	−8.6	2.1	−21.3	−18.4
O_w–H_w–C_2–C_1	2.5	12.6	13.1		3.2	−1.4		35.4	19.7	−83.7	−86.4	−87.2
H_w–C_2–C_1–N_3	−26.1	−40.8	−41.0	32.6[h]	32.6[i]	34.0[i]	8.4[h]	27.8[i]	33.1[i]	63.9	56.5	56.6
N_3–C_1–C_2–C_R[j]	93.0	75.1	76.5	−61.6	−81.8	−83.2	−32.0	−92.5	−92.7	174.9	177.1	176.8

[a] Complete structures are available upon request from the authors. [b] O_5H_3. [c] O_5H_w. [d] O_wO_5. [e] $O_wH_wO_5$. [f] $H_3O_tC_4$. [g] $H_wO_5C_4$. [h] $H_3O_5C_4C_2$. [i] $H_wO_5C_4C_2$. [j] C_R is the carbon of the R group attached to C_2.

of a general base in the abstraction of a proton from the protonated amine of the zwitterionic form to yield the conjugated anion which could be stabilized by resonance with the group R on C_α. Subsequently, a general acid is required to convert the anionic form to products by donating a proton to the carbanion. Nucleophilic addition of ammonia to an activated double bond of ACR, ACN, or AA requires the formation of a transient zwitterionic interaction complex **2** (Scheme I). In a computational simulation of the formation of **2** in vacuum, we observed that the interaction is monotonically repulsive for distances between C_1 and N_3 (see Scheme I for numbering of atoms) ranging from 3.0 to 1.5 Å. An attempt to calculate the stabilization of the zwitterionic form by a polar solvent, such as water, also resulted in an unfavorable state relative to the separated molecules. Taken together, these findings and considerations lead to the hypothesis that in the process of ammonia addition to an activated double bond, the aqueous solution provides not only a polar medium for the reaction but also a discrete water molecule that participates in the reaction. The reaction path is shown in Scheme II and represents the nucleophilic 1,2-addition of an amine assisted by a discrete water molecule. The role of the explicit water molecule in this mechanism is to act as a shuttle for the proton between N_3 and C_2 and is thus added to the effect of bulk solvent computed here from a model of continuum dielectric (see below).

The potential energy surface for the 1,2-nucleophilic addition of $NH_3{\cdot}OH_2$ to an activated double bond in ACN was scanned with the semiempirical AM1 method. Results are shown in Figure 1. The nucleophilic attack of ammonia is characterized by (i) the C_1–N_3 distance to the attacked carbon, (ii) the N_3–H_3 distance of the hydrogen bond between ammonia and the water molecule, and (iii) the C_2–H_w distance of the nascent bond to the second carbon of the double bond (see Scheme II for numbering of atoms). Results in Figure 1 show that two of the internal coordinates, N_3–H_3 and C_2–H_w, are coupled to their complementary internal coordinates, the H_3–O_w and the O_w–H_w distances, respectively. The energetic relationships among the various positions in the reaction path are reflected in the potential energy surface constructed from the energies of the movement of the protons (H_3 and H_w) for fixed C_1–N_3 distances of 2.0, 1.8, 1.6, and 1.445 Å (the C_1–N_3 distance of 1.445 Å represents the optimized bond in the products of addition to ACN).

1. Transition-State Structures. For the nucleophilic addition of $NH_3{\cdot}OH_2$ to the activated double bonds of ACR, AA, and ACN, transition states were identified, as described in the Methods

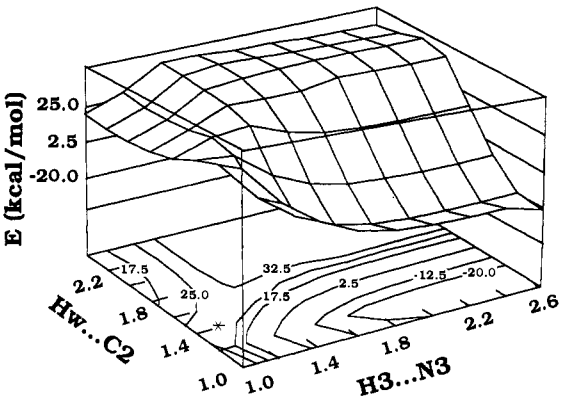

Figure 1. Semiempirical potential energy surface, calculated with the AM1 Hamiltonian, of the 1,2-nucleophilic addition of $NH_3{\cdot}OH_2$ to the reactive double bond of acrylonitrile. The potential energy surface is calculated at a fixed C_1–N_3 distance of 1.445 Å. The distance C_2–H_w is represented on the *x*-axis and the N_3–H_3 distance on the *y*-axis. The energy contours (in kcal/mol) represent values relative to the separated ACN and $NH_3{\cdot}OH_2$. The TS (identified by the asterisk) has the proton near C_2. After the TS, the H_3 proton of ammonia approaches the water molecule (the direction of increasing H_3··N_3 values).

section, from ab initio calculations of the potential energy surface around the structures initially identified from the AM1 calculations. The resulting structures were further optimized with the 6-31G basis set employing analytical gradient procedures. The harmonic vibrational frequencies characterize these stationary points as real TS in which the matrices of force constants have a single negative eigenvalue. The major contribution to the eigenvector with the negative eigenvalue comes from C_2–H_w, a minor contribution comes from the C_1–N_3 internal coordinate, and no significant contribution comes from the N_3–H_3 internal coordinate. These structures are consistent with the accepted mechanisms of nucleophilic addition to activated double bonds[19] and are very similar to the cyclic, activated complexes identified by Williams[24] from similar studies on the attack of a C=O bond. The most relevant geometrical parameters of the optimized TS **5** and products **6** are given in Table I and depicted in Figures 2 and 3, respectively.

The optimized TS of **5** for ACR, AA, and ACN are very similar in the internal coordinates that contribute to the reaction path: C_1–N_3, N_3–H_3, and C_2–H_w (see Table I and Figure 2). With the

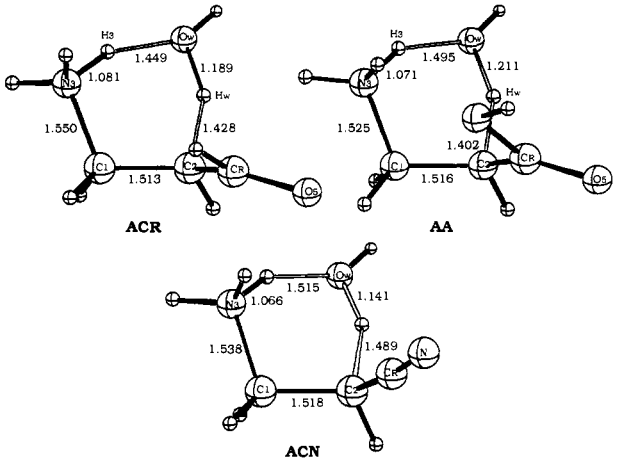

Figure 2. Optimized transition-state structures (**5**, see Scheme II) of the nucleophilic 1,2-addition of $NH_3{\cdot}OH_2$ to ACR, AA, and ACN at the HF/6-31G level of theory.

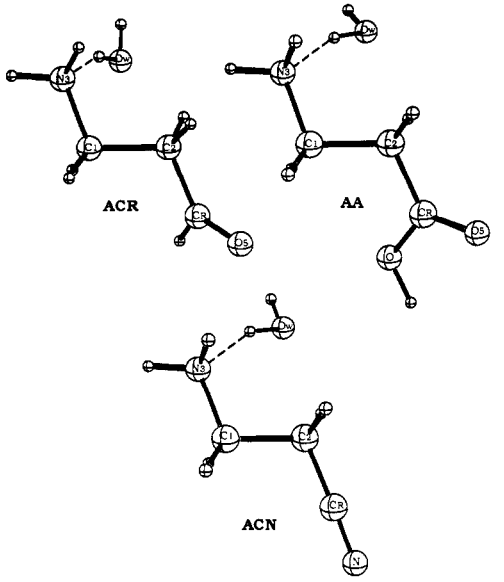

Figure 3. Optimized equilibrium products of the nucleophilic 1,2-addition (**6**, see Scheme II) and 1,4-addition (**6**, see Scheme IIIb) of $NH_3{\cdot}OH_2$ to ACR, AA, and ACN at the HF/6-31G level of theory.

exception of C_1–N_3, which has a minor contribution to the reaction coordinate at the TS, there is no correlation between the values of the internal coordinates and the barriers for the process (see Table IV) described by Scheme II. This behavior is especially noteworthy because the major contribution to the reaction coordinate at the TS comes from the C_2–H_w bond, which clearly does not correlate with the barrier. An analysis of the TS yields a description of the mechanism of the nucleophilic 1,2-addition of $NH_3{\cdot}OH_2$ to the double bond of ACR, AA, and ACN in terms of electronic and structural changes.

The initial approach to the $NH_3{\cdot}OH_2$ complex to C_1 is at an incident N–C_1–C_2 angle of ca. 110° in a plane nearly perpendicular to the C_1–C_2–C_R plane (C_R is the carbon of the R group attached to C_2). The orientation dihedral angle N_3–C_1–C_2–R for ACR, AA, and ACN is 93.0°, 75.1°, and 76.5°, respectively (see Table I). Along this approach, the energy increases monotonically until the C_1–N_3 distance reaches an approximate value of 1.5 Å (see C_1–N_3 values of structure **5** in Table I and Figure 2). Due to the approach of the $NH_3{\cdot}OH_2$ complex, C_1 and C_2 are pyramidalized, the charge density of the TS is polarized, and C_2 acquires negative charge following the attack of NH_3 on C_1 (see Figure 2). Selected values of Mulliken charges of heavy atoms, with hydrogen charges summed into them, are shown for the reactants and for the TS

Table II. Selected Values of Mulliken Charges[a] of the Reactants (**1** and **4**) and Transition States for the 1,2- (**5**) and 1,4-Nucleophilic (**7**) Michael Addition to ACR, AA, and ACN, Calculated with the 6-31G* Basis Set

species		C_1	C_2	C_R	O_5	N_3	O_w
1 and **4**	ACR	0.04	0.00	0.48	−0.51		
	AA	0.10	−0.03	0.77	−0.59		
	ACN	0.10	0.07	0.28	−0.45		
	$NH_3{\cdot}{\cdot}OH_2$					−0.01	0.01
5	ACR	0.24	−0.43	0.47	−0.59	0.44	−0.13
	AA	0.25	−0.45	0.84	−0.63	0.47	−0.11
	ACN	0.26	−0.41	0.32		0.47	−0.11
7a	ACR	0.28	−0.28	0.45	−0.72	0.26	
7b	ACR	0.23	−0.25	0.46	−0.83	0.44	−0.05
	AA	0.23	−0.27	0.80	−0.86	0.43	−0.05

[a] Atomic charges with hydrogens are summed into heavy atoms.

Table III. Total Energies (hartrees), ZPE (kcal/mol), and E_{solv} (kcal/mol) of the Reactants (**1** and **4**), the Transition States for the 1,2- (**5**) and 1,4-addition (**7**), the Intermediates (**8**), and the Products (**3** and **6**) of the Nucleophilic Michael Addition to ACR, AA, and ACN

species		HF/6-31G	MP2/6-31G*	ZPE	E_{solv}
1 and **4**	ACR	−190.67776	−191.31026	41.9	−11.0
	AA	−265.53339	−266.37727	45.7	−13.2
	ACN	−169.69392	−170.29490	34.6	−10.0
	NH_3	−56.16552	−56.34819	22.8	−8.0
	$NH_3{\cdot}{\cdot}OH_2$	−132.15644	−132.54962	38.5	−12.8
3	ACR	−246.85625	−247.68664	69.1	−12.2
	AA	−321.71501	−322.75677	73.0	−14.9
	ACN	−225.88021	−226.67663	61.9	−10.1
5	ACR	−322.77952	−323.82728	83.3	−24.3
	AA	−397.65114	−398.90752	87.9	−27.7
	ACN	−301.80349	−302.81920	76.7	−20.3
6	ACR	−322.85517	−323.89918	85.9	−19.1
	AA	−397.71304	−398.96891	89.7	−25.3
	ACN	−301.87775	−302.88898	78.9	−16.5
7a	ACR	−246.80656	−247.63724	69.1	−16.4
7b	ACR	−322.82663	−323.86051	84.1	−20.8
	AA	−397.67215	−398.91422	86.8	−23.6
8a	ACR	−246.85303	−247.67489	70.6	−11.2
8b	ACR	−322.85535	−323.88586	87.5	−16.1
	AA	−397.69181	−398.93062	90.5	−19.2

in Table II. Clearly, the charge on C_2 changes from neutral in the reactants (e.g., **4**) to −0.43, −0.45, and −0.41 for ACR, AA, and ACN in the TS **5**, respectively. In parallel, the charge on N_3 changes from neutral to positive. The attraction of the water molecule by the negative charge on C_2 brings H_w to the proximity of C_2 by bending the previously linear N_3–$H_3{\cdot}{\cdot}O_w$ hydrogen bond (see Table I). An important consequence of this structural change is a significant stretch of the O_w–H_w bond while the N_3–H_3 bond remains nearly unchanged (see values of structure **5** in Table I and Figure 2). These findings suggest that the movement of H_w from the water to C_2 occurs at an earlier stage along the reaction coordinate than the movement of H_3 from ammonia to water. The sequential movement of both protons (H_3 and H_w) leads to the products of the nucleophilic addition. Thus, we find that the *minimum reaction path involves the attack of the proton of the water molecule on the negative charge generated on C_2 due to the nucleophilic attack of ammonia on the reactive double bond. From this point, the movement of H_3 from ammonia to water is energetically a downhill process.*

2. Energetics of the 1,2-Nucleophilic Addition. Single-point calculations were performed at the MP2 level with the 6-31G* basis set. Total energies at the various levels of theory along with the ZPE and E_{solv} are summarized in Table III. The energies relative to reactants **4** of the optimized TS **5** (E_{act}) and of products **6** (E_{react}) are given in Table IV. All the reactions are exothermic with E_{react} in the range of 20 kcal/mole when calculated at the MP2/6-31G* level and corrected for ZPE. The barriers to the 1,2-nucleophilic addition, calculated at the HF/6-31G level of

Table IV. Energies (kcal/mol) Relative to Reactants (**1** and **4**) of the Optimized Transition States (**5**, 1,2-addition; **7**, 1,4-addition), Intermediates (**8**), and Products (**6**) of the Nucleophilic Michael Addition of Ammonia (Scheme IIIa) or NH_3·OH_2 (Scheme II and IIIb) to ACR, AA, and ACN

species			HF/ 6-31G	MP2/ 6-31G*	MP2/ 6-31G* +ZPE	MP2/ 6-31G* +ZPE +E_{solv}
			Scheme II			
5	E_{act}	ACR	34.3	20.4	23.4	22.9
		AA	24.3	12.1	15.8	14.1
		ACN	29.4	15.9	19.5	22.0
6	E_{react}	ACR	-13.2	-24.7	-19.1	-14.4
		AA	-14.6	-26.4	-20.8	-20.1
		ACN	-17.2	-28.5	-22.7	-16.4
			Scheme IIIa			
7a	E_{act}	ACR	23.0	13.3	17.7	19.3
8a	E_{inter}	ACR	-6.1	-10.3	-4.4	2.4
3	E_{react}	ACR	-8.1	-17.7	-13.3	-7.5
			Scheme IIIb			
7b	E_{act}	ACR	4.7	-0.4	3.4	6.4
		AA	11.1	7.9	10.5	12.9
8b	E_{inter}	ACR	-13.3	-16.3	-9.2	-1.5
		AA	-1.2	-2.3	3.9	10.7
6	E_{react}	ACR	-13.2	-24.7	-19.1	-14.4
		AA	-14.6	-26.4	-20.8	-20.1

Scheme III[a]

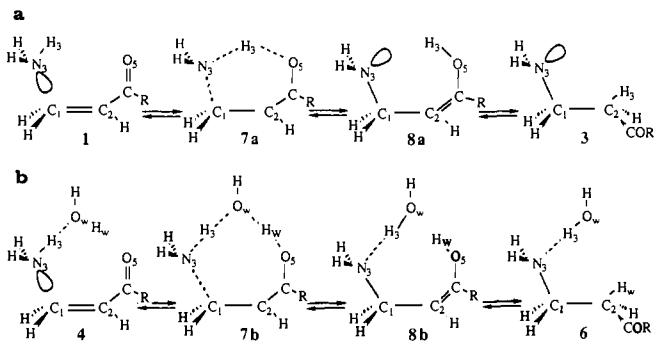

[a] R = H and OH.

theory, are very high ranging from 24.3 kcal/mol for AA to 34.3 kcal/mol for ACR. The same barriers calculated with MP2/6-31G* and corrected for ZPE are found to decrease considerably, approximately by 10 kcal/mol, to 23.4, 15.8, and 19.5 kcal/mol for ACR, AA, and ACN, respectively. The predicted order of reactivities, based on energies of activation, would be AA > ACN > ACR. These results are not in agreement with the rank order of reactivity observed experimentally.[15] Although inclusion of solvation energies in the calculated energies of activation tends to stabilize the TS of ACR and AA, it destabilizes the TS of ACN so that the rank order of reactivities remains the same (see Table IV). *We conclude that the differences in reactivities of ACR, AA, and ACN can not be explained by the parameters obtained from the potential energy surfaces of the nucleophilic 1,2-addition.*

Nucleophilic 1,4-Addition. The presence of carbonyl groups in compounds with activated double bonds, such as ACR or AA, gives rise to a possibility that the Michael reaction will proceed through a 1,4-addition mechanism. In such a situation, two other mechanistic pathways for the intramolecular proton transfer from N_3 to C_2 are possible (Scheme III). One involves the ammonia alone (Scheme IIIa), which acts as the nucleophile and the proton donor to O_5. The other pathway simulates the attack of a NH_3·OH_2 (Scheme IIIb), in which the water molecule acts as a shuttle of the proton from the NH_3 to O_5. The *s-cis* conformations of the conjugated carbonyl of ACR or AA allow for the possibility of the movement of the proton from N_3 to the oxygen of the

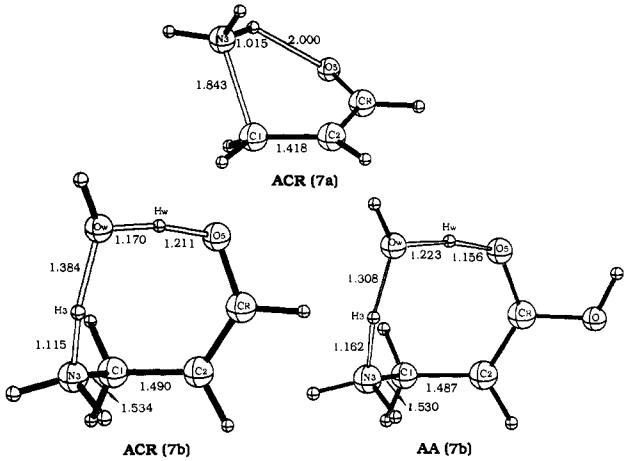

Figure 4. Optimized transition-state structures of the nucleophilic 1,4-addition of either ammonia (**7a**, see Scheme IIIa) or NH_3·OH_2 (**7b**, see Scheme IIIb) to ACR and AA.

carbonyl group (O_5) through a cyclic transition structure (**7**) in which both ends of the conjugated system interact with the nucleophilic reagent. This yields a *cis*-enol intermediate (**8**) which, after a 1,3-tautomeric keto–enol shift, produces the same product **6** as the 1,2-addition mechanism. This type of the 1,4-addition has been suggested for the nucleophilic addition of organocopper reagents to ACR.[31]

1. Transition-States Structures. The transition-state structures of the 1,4-nucleophilic addition of either ammonia (Scheme IIIa) or NH_3·OH_2 (Scheme IIIb) to ACR are shown in Figure 4. The calculated harmonic vibrational frequencies confirm that these stationary points are real transition states. The matrices of force constants of both TS **7a** and **7b** have a single negative eigenvalue. The major contribution to the eigenvector with the negative eigenvalue of the Hessian matrix of **7a** comes only from the C_1–N_3 internal coordinate; there is no significant contribution from the N_3–H_3 internal coordinate. A different behavior is found in the matrix of force constants of **7b**. The O_5–H_w and N_3–H_3 internal coordinates are the major components of the eigenvector of the Hessian matrix with the negative eigenvalue, and the C_1–N_3 makes no significant contribution. Structural parameters of the optimized TS structures **7a** and **7b** are shown in Table I.

The most salient geometrical difference between TS **7a** and **7b** for ACR is the unequal value of the C_1–N_3 reaction coordinate. The TS of the nucleophilic attack of ammonia in the absence of water (**7a**) occurs at a C_1–N_3 distance of 1.843 Å (see Table I and Figure 4). At this point, H_3 did not yet start its movement toward O_5, as is indicated by the N_3–H_3 distance of 1.015 Å. When the TS of the nucleophilic attack is calculated in the presence of the water molecule (**7b**), the C_1–N_3 bond is almost completely formed with a value of 1.534 Å. Table III lists the total energies, ZPE, and E_{solv} for these structures, and Table IV contains the activation energies relative to the *s-trans* conformation of ACR. At the MP2/6-31G* level of theory corrected for ZPE, the E_{act} for the 1,4-addition of ammonia in the absence of water (see structure **7a** in Table IV) is 17.7 kcal/mol. At the same level of theory, the barrier for the 1,4-addition in the presence of the discrete water molecule is found to be only 3.4 kcal/mol (see **7b** in Table IV). The large preference of the TS **7b** over the TS **7a** could be associated with a better stabilization of the charge distribution in the TS by the additional water molecule that bridges between the positively charged NH_3 and the negatively charged O_5. Furthermore, the hydrogen-bond distances, N_3··H_3··O_w and O_w··H_w··O_5, in structure **7b** are much shorter and less strained than the corresponding N_3··H_3··O_5 hydrogen-bond distance in **7a** (see Table I).

(31) Dorigo, A. E.; Morokuma, K. *J. Am. Chem. Soc.* **1989**, *111*, 4635–4643.

Due to the large difference in activation energy found for the two reaction paths, only the 1,4-addition in presence of the water molecule (Scheme IIIb) was calculated for AA. The major components of the eigenvector of the Hessian matrix with the negative eigenvalue are very similar to those for ACR. The transition-state structure is shown in Figure 4, and the geometrical parameters are listed in Table I. The 1,4-nucleophilic addition to AA can be described as follows. The approach to C_1 of ammonia hydrogen bonded to a discrete water molecule converts the atoms forming the reactive double bond into nearly tetrahedral carbons. The presence of ammonia causes a negative charge density to be shifted in the conjugated double bond, with a major concentration on O_5. Because oxygen is more electronegative than carbon, this negative charge is better accommodated in this mechanism than in the 1,2-addition to the carbon–carbon double bond (Scheme II). This fact is reflected in the Mulliken charges of the heavy atoms listed in Table II. The charge on O_5 for **7b** is –0.83 and –0.86 for ACR and AA, respectively, while the charge on C_2 in **5** is only –0.43 and –0.45 for the same compounds. The more negative charge density on O_5 facilitates the attraction of H_w to O_5, leading to a TS in which the distance O_5–H_w is significantly shorter than C_2–H_w in the 1,2-addition (1.211 Å vs 1.428 Å for ACR and 1.156 Å vs 1.402 Å for AA, see Table I and Figures 2 and 4). At the same time, C_1–N_3 remains very similar to that in the 1,2-addition mechanism (1.534 Å vs 1.550 Å for ACR and 1.530 Å vs 1.525 Å for AA, see Table I and Figures 2 and 4). Thus, the susceptibility of C_1 to nucleophilic attack is approximately the same in both the 1,2- and the 1,4-addition mechanisms, but the electrostatic stabilization of the O_w··H_w··O_5 hydrogen bond compared to O_w··H_w··C_2 is responsible for the different activation energies in these two processes (see below). Furthermore, analysis of the structural parameters (Table I) of transition structures **5** and **7b** reveals another important difference. In the 1,2-addition, the movement of H_w from the water to C_2 occurs at an earlier stage along the reaction coordinate than the movement of H_3 from ammonia to water; in the 1,4-addition, both H_3 and H_w are almost midway in their movement to O_w and O_5, respectively (see N_3–O_w, H_3–H_3, O_w–O_5, and O_5–H_w distances of structure **7b** in Table I and Figure 4). *Therefore, the minimum reaction path of the proton movement from N_3 to O_5 takes advantage of a concerted mechanism in which H_3 moves toward O_w and H_w moves from O_w to O_5. Thus, the discrete water molecule acts as a catalyst in this proton rearrangement, contributing primarily to the lowering of the barrier to the proton shuttle.* The optimized reaction coordinates that contribute to the 1,4-reaction path, N_3–H_3 and O_5–H_w, are essentially identical in AA and ACR. However, at similar N_3–O_w and O_w–O_5 distances, the positions of the protons H_3 and H_w are closer to the proton-acceptor atoms O_w and O_5 in AA than in ACR (see O_5–H_w and N_3–H_3 distances in structure **7b** in Table I). This indicates that the TS of ACR occurs somewhat earlier along the reaction coordinate.

After the TS is reached, a concerted mechanism of proton rearrangement yields an enol intermediate, **8** (Figure 5). It is interesting to point out that **8b** is stabilized by a ring structure which includes the hydrogen bonds N_3··H_3–O_w and O_w··H_w–O_5 (see Figure 5 and Scheme IIIb) with interatomic hydrogen-bond distances of 2.739 and 2.675 Å for ACR and 2.712 and 2.608 Å for AA (see Table I). Finally, **8** undergoes the 1,3-shift of the keto–enol tautomerism, yielding the same product **6** as the 1,2-addition mechanism.

2. Energetics of the 1,4-Addition. The total energies obtained at the various levels of theory, ZPE and E_{solv} of the TS **7** and the intermediate **8**, are summarized in Table III. The energies relative to reactants (**1** for Scheme IIIa and **4** for Scheme IIIb) of the optimized TS **7** (E_{act}) and intermediates **8** (E_{inter}) are given in Table IV. At the highest level of theory employed here (MP2/6-31G*) and corrected for the ZPE, the barrier to 1,4-nucleophilic addition is 3.4 kcal/mol for ACR and 10.5 kcal/mol for AA. Inclusion of the contribution of solvation to the calculated barriers increases the values to 6.4 and 12.9 kcal/mol for ACR and AA, respectively. Notably, the energy of activation for AA is considerably higher than for ACR, despite the fact that the initial structure of the reactant AA is already the *s-cis,syn* conformation and ACR must produce a conformational change from *s-trans* to *s-cis* along the reaction path. This conformational change is estimated to be of the order of 1.7 kcal/mol.[28] This behavior would be consistent with the larger resonance effect of the CHO group in ACR than that of the COOH group in AA.

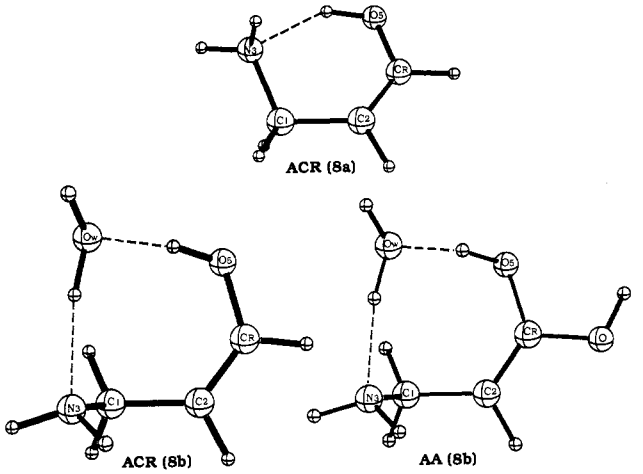

Figure 5. Optimized intermediate structures of the nucleophilic 1,4-addition of either ammonia (**8a**, see Scheme IIIa) or NH_3·OH_2 (**8b**, see Scheme IIIb) to ACR and AA.

In order to resolve the apparent discrepancy between the barrier size and the similar charge distribution, it would be instructive to compare the intrinsic barriers (E_{act}*) for these reactions. An intrinsic barrier can be considered as the barrier that a reaction would have in the absence of a thermodynamic driving force,[32] and, thus, it would not be affected by the relative stability of the immediate products of the reaction, i.e., the energies of the intermediates before the 1,3-proton shift. The intermediate **8b** of ACR, formed in the 1,4-addition, is stabilized by –9.2 kcal/mol, as is indicated by its E_{inter}, but the intermediate of AA is destabilized by 3.9 kcal/mol with respect to reactants at the MP2/6-31G*+ZPE level of theory. Taking these results into account and recalculating the intrinsic barriers according to the equation[32]

$$E_{act} = [(E_{inter})^2/16E^*_{act}] + E^*_{act} + {}^1/_2E_{inter}$$

yields the following values: 7.23 kcal/mol for ACR and 8.46 kcal/mol for AA. Clearly, the stabilization of the intermediate **8b** of ACR increases the intrinsic barrier, and the destabilization of the intermediate of AA lowers the barrier. The final result is that the intrinsic barriers are nearly equal, which is in agreement with the similar structures of the TS and their charge distribution.

Inclusion of solvation tends to increase the barriers and destabilize the intermediate structures. This in turn lowers the intrinsic barriers to 7.09 kcal/mol for ACR and 6.47 kcal/mol for AA, bringing their values to a closer agreement. However, the intermediate structure of ACR remains stable with respect to the reactants by –1.5 kcal/mol, while the intermediate formed for AA is unstable by 10.7 kcal/mol. Notably, a similar enol intermediate, **8a**, is obtained in the 1,4-addition of ammonia to ACR without the participation of a discrete water molecule (Scheme IIIa). The intermediate **8a** was found to be unstable by 2.4 kcal/mol with respect to reactants when both correlation and solvation energies were included in the calculation (see E_{inter} for structure **8a** on Table IV). This indicates that the water

(32) *Nucleophilicity*: Harris, J. M., McManus, S. P., Eds.; American Chemical Society: Washington, D.C., 1987; Vol. 215.

molecule plays another important role in the 1,4-addition mechanism. In addition to catalyzing the movement of a proton from N_3 to O_5, the water molecule stabilizes the enol intermediate through the two hydrogen bonds $N_3 \cdots H_3-O_w$ and $O_w \cdots H_w-O_5$ (see Figure 5, Scheme IIIb, and above).

It is quite evident from the values in Table IV (see E_{act} of structures **5** and **7b**) that energetically the most likely mechanism of the nucleophilic addition of ammonia to the conjugated double bond of ACR is the 1,4-addition assisted by a discrete water molecule (Scheme IIIb). The difference in activation energy between the 1,2- and 1,4-addition mechanisms to ACR is found to be 16.5 kcal/mol when correlation, ZPE, and solvation energy are included in the calculation. In contrast, the differences observed between the two mechanisms for addition to AA are much smaller. At the MP2/6-31G*+ZPE+E_{solv} level of theory, the barriers for the 1,2- and 1,4-addition to AA are 14.1 and 12.9 kcal/mol, respectively (see Table IV). With such a small difference in E_{act}, the chemical nature of the nucleophile and the relatively small electrostatic effect of the environment in which the reaction occurs could change the preference of addition to AA from the 1,4- to the 1,2-mechanism. However, the new predicted order of reactivities, based on energies of activation of the 1,4-addition to ACR, either 1,2- or 1,4-addition to AA, and 1,2-addition to ACN, would qualitatively reproduce the rank order of reactivity: ACR > AA > ACN, which is in very good agreement with experimental results.[11]

Conclusions

The present study of the molecular mechanism of nucleophilic addition of ammonia to the activted double bond in ACR, AA, and ACN indicates that the addition proceeds through the formation of a transition state in which the rate-determining step is an intramolecular proton transfer from the nucleophile to the ligand, assisted by a discrete water molecule which acts as a catalyst of this process (cf. results in ref 24 where the catalysis by a H_2O molecule was shown to arise from the increase in hydrogen bonding to the zwitterion-like moiety in the activated complex). Notably, the molecular mechanism by which either ACR or AA takes part in this process is different from that observed here for ACN. The *s-cis* conformation of the carbonyl groups of ACR or AA allows for the possibility of a nucleophilic 1,4-addition. In the TS of this addition, the intramolecular proton transfer proceeds from the nucleophile to the O_5 oxygen of ACR or AA via the discrete water molecule through a *concerted mechanism* in which both protons H_3 and H_w are midway in their movement. The 1,4-addition is not possible for ACN because of the linearity of the cyano group. The 1,2-addition to ACN comprises the intramolecular proton transfer from the nucleophile to the C_2 carbon of ACN via the discrete water molecule through a *sequential mechanism* in which the water molecule first donates a proton to the negative charge generated on C_2 and subsequently abstracts the H_3 proton from ammonia. The structural preference observed for the 1,4-mechanism is due to the electrostatic stabilization of the TS by the high negative charge on the terminal oxygen of the carbonyl conjugated to the double bond. By comparison, the charge on the carbon of the double bond is much smaller, resulting in less stabilization of the TS.

As it has been proposed that a Michael-type addition is a primary event in the mechanism of interaction between chemicals in the class of enals and biological nucleophiles that leads to their observed biological effects (see refs 1 and 33), it is attractive to assume that the same relative preferences identified here for the nucleophilic addition of ammonia to representaive species in the class of molecules with actívated double bonds should govern their reactivities toward larger, nitrogen-containing target groups in biopolymers. The intramolecular proton shuttle may be assisted by the biomolecule, such as DNA or another species with nucleophilic sites.

Acknowledgment. This work was supported in part by the U.S. Enviromental Protection Agency under cooperative research agreement CR-814292. H.W. is a recipient of a Research Scientist Development Award (DA-00060) from the National Institute of Drug Abuse. Some of the computations were performed at the National Computer Center of the Environmental Protection Agency. Generous grants of computer time from the Advanced Scientific Computing Laboratory at the Frederick Cancer Research Facility of the National Cancer Institute (Laboratory for Mathematical Biology) and from the University Computer Center of the City University of New York are gratefully acknowledged. The research described in this paper has been reviewed by the Health Effects Research Laboratory of the U.S. Environmental Protection Agency and approved for publication. Approval does not signify that the contents necessarily reflect the views and policy of the agency nor does mention of trade names or commercial products constitute endorsement or recommendation for use.

(33) Dearfield, K. L.; Harrington-Brock, K.; Doerr, C. L.; Rabinowitz, J. R.; Moore, M. M. *Mutagenesis* **1991**, *6*, 519–525.